

Cite this: *Chem. Sci.*, 2012, **3**, 1938

www.rsc.org/chemicalscience

EDGE ARTICLE

# Catalytically active supramolecular porphyrin boxes: acceleration of the methanolysis of phosphate triesters *via* a combination of increased local nucleophilicity and reactant encapsulation†

Byungman Kang, Josh W. Kurutz, Kyoung-Tae Youm,‡ Ryan K. Totten, Joseph T. Hupp\* and SonBinh T. Nguyen\*

Received 21st November 2011, Accepted 25th January 2012

DOI: 10.1039/c2sc00950a

Box-like tetrakis(metalloporphyrin) supramolecular assemblies possessing Zn and Al metal sites can catalyze the methanolysis of phosphate triesters with a high rate enhancement, up to 430 times faster than the uncatalyzed reaction. Mechanistic studies suggest that the observed rate enhancement can be attributed to a high local concentration of methoxide ion that operates in concert with a solvophobic driven encapsulation of substrates by the porphyrinic assembly.

## Introduction

A broad range of strategies has been used in designing supramolecular structures that exhibit catalytic potency exceeding those of the isolated molecular components.<sup>1–4</sup> Among the supramolecular assemblies that have been investigated for catalysis, those based on metalloporphyrins have been among the most popular.<sup>5,6</sup> The attractiveness of porphyrin lie in its rigidity, tunable periphery, and structural similarity to cofactors (such as heme groups) essential for catalysis by many metalloenzymes.<sup>7</sup> While coordinative self-assembly has been used to create topologically well-defined and active site-isolated supramolecular catalysts based on metalloporphyrins,<sup>8–11</sup> these systems often rely on weak coordinative interactions that are not stable in polar solvents or at high temperatures. As such, many researchers<sup>12–14</sup> have begun to explore the use of more stable, covalently linked cyclic multiporphyrin assemblies in supramolecular catalysis. Since the metalloporphyrins are permanently linked in such structures, catalysis with Lewis-basic, coordinating substrates can be affected without concern for the stability of the assembly. For example, pyridine- and imidazole-containing substrates have been pre-organized into optimal transition-state-like geometries for acyl transfer<sup>12</sup> and Diels–Alder<sup>15</sup>

reactions using the metal centers in covalently linked tris(porphyrin) assemblies, leading to substantial reaction rate enhancements.

We<sup>16</sup> and others<sup>17–19</sup> have demonstrated the facile preparation of covalently linked hollow metalloporphyrin assemblies using templated ring-closing metathesis (tRCM). This versatile strategy can serve as a general route to a multitude of synthetic multiporphyrin hosts with tunable cavity size from a single modular building block. Furthermore, because the tRCM linkage chemistry is compatible with a wide range of porphyrin modification chemistries, such synthetic hosts can readily be tuned to engender supramolecular recognition capabilities and catalysis activities that are not expressed in single-porphyrin systems. Beyond the transition-state-stabilization effect that had been explored for accelerating bimolecular reactions,<sup>12,15</sup> we were intrigued by the possibility that the multi-metallic environment within a polyporphyrin cavity could also lead to increased local concentration of a metal-ligating reagent inside the cavity and thus further increases in reaction rate, similar to that observed recently in a porphyrin-containing metal–organic framework.<sup>20</sup>

In addition to coordination and hydrogen bonds, van der Waals forces and solvophobic effects can also play key roles in enzyme catalysis through attractive noncovalent interactions that stabilize transition states and lower kinetic barriers to reactions.<sup>21</sup> Without the need for covalent bonds, a combination of these interactions can allow a host cavity to bring reactants together at an active site in a conformation that is close to the transition state of a reaction. For example, a highly hydrophobic host molecule such as a multiporphyrin assembly can interact favorably with a hydrophobic substrate in aqueous media, essentially “encapsulating” it inside the cavity. Together with the aforementioned “increased local concentration effect” of a metal-ligating reagent, this “solvophobic substrate encapsulation” can work synergistically to increase reaction rates. To test

Department of Chemistry and International Institute for Nanotechnology, Northwestern University, 2145 Sheridan Road, Evanston, IL, 60208, USA. E-mail: j-hupp@northwestern.edu; stn@northwestern.edu; Fax: +1 847 491-7713; +1 847-467-1425; Tel: +1 847-467-3347; +1 847-491-3504

† Electronic supplementary information (ESI) available: Complete experimental details of syntheses; compound characterization data and spectra; PFG NMR/titration experimental methods, spectra, and data analysis; computational estimates of methoxide concentrations, EM, and binding constants; as well as detailed description of catalytic conditions and results of the methanolysis. See DOI: 10.1039/c2sc00950a

‡ Current address: Samsung Cheil Industries Inc., Uiwang, Gyeonggi 437-711, Republic of Korea.

this hypothesis, we chose the bimolecular methanolysis of phosphate triesters in a concentrated methanol environment as a test model. As substrates, aromatic phosphate triesters are ideal for this type of investigation: they have weak Lewis basicity and do not bind strongly to the metalloporphyrin under high MeOH concentrations, thus allowing for facile turnover. Furthermore, one can envision their hydrophobic aromatic substituents interacting well with the hydrophobic, aromatic plane of the porphyrin.

Herein, we report a large rate acceleration for the methanolysis of phosphate tri(aryl esters) catalyzed by a tetrakis(methoxyaluminum porphyrin) assembly, that can be attributed to a combination of enhanced local methoxide concentration and solvophobic substrate binding. By incorporating nucleophilic Al-OMe centers into a hydrophobic tetrakis(porphyrin) assembly, a cavity containing a high concentration of methoxy ligands is created that enhance the methanolysis of a solvophobically encapsulated phosphate triester. Such an environment would not be available in reactions catalyzed by either the analogous tetrakis(zinc porphyrin) assembly or by the (methoxyaluminum porphyrin) monomer, which are expected to yield only modest rate enhancements.

## Results and discussion

### Synthesis and characterization of metalloporphyrin boxes

The syntheses of covalently linked hollow tetrakis(metalloporphyrin) boxes (**(Zn-PP)<sub>4</sub>**) and (**(MeO-Al-PP)<sub>4</sub>**) are outlined in Scheme 1. Our modular design allows for the facile synthesis of two distinct robust metalloporphyrin assemblies from a single porphyrin building block (**Zn-PP**), [[5,15-bis(4-(1-pentenyl)oxy)phenyl]-10,20-bis((trihexylsilyl)ethynyl)]porphyrato]zinc(II) in *three steps or less*. The judicious incorporation of the *meso*-trihexylsilyl ethynyl substituents into the porphyrin monomers allows these building blocks and the assembled (**Zn-PP)<sub>4</sub>** and (**(MeO-Al-PP)<sub>4</sub>**) tetramers to remain soluble in common solvents such as methylene chloride, chloroform, toluene, and tetrahydrofuran. In the presence of 0.25 equiv of the tetrakis(4(4'-pyridyl)-3,5-dimethylphenyl)porphyrin (**Py-MesP**) template and Grubbs second-generation catalyst<sup>22</sup> (35 mol%), **Zn-PP** monomer (0.5 mM) readily undergoes tRCM to afford the covalently

linked, templated tetramer (**(Zn-PP)<sub>4</sub>·(Py-MesP)**) in 74% yield. The <sup>1</sup>H NMR spectrum of this product differs significantly from those for **Zn-PP** and the **Py-MesP** template (Fig. 1). The appearance of broad singlets at 5.75 and 5.87 ppm (1 : 9 ratio, Fig. 1c), attributed to the *E* and *Z* isomers of internal olefin linkages, respectively, support the covalently linked nature of the assembly.<sup>17–19</sup> In addition, the  $\alpha$  and  $\beta$ -pyridyl protons of the encapsulated **Py-MesP** template display substantial upfield shifts (2.74 and 7.50 ppm) (*cf.* Figs. 1a and c), indicative of a strongly shielded environment and consistent with coordination of the pyridyl groups by Zn(porphyrin) centers.<sup>23,24</sup>

For the ring-closing reactions to proceed to completion, the size of the template should match well with that of the corresponding box: formation of the covalently linked (**Zn-PP)<sub>4</sub>** structure was not observed by matrix-assisted laser desorption/ionization time-of-flight (MALDI-ToF) mass spectrometry when the assembly was attempted with the smaller template, 5,10,15,20-tetrakis(4-pyridyl)porphyrin. Hollow (**Zn-PP)<sub>4</sub>** can be readily obtained from the templated (**(Zn-PP)<sub>4</sub>·(Py-MesP)**)

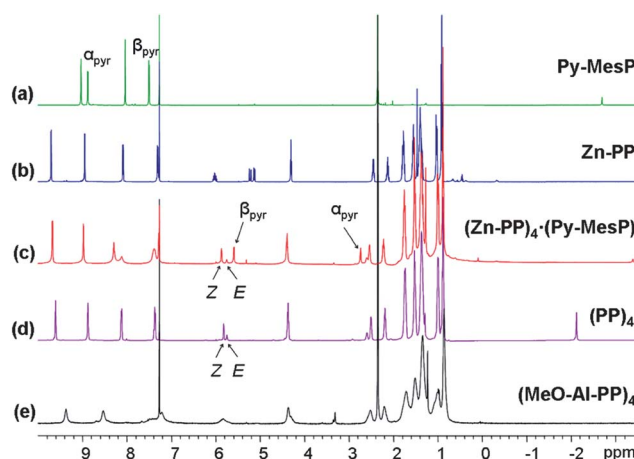
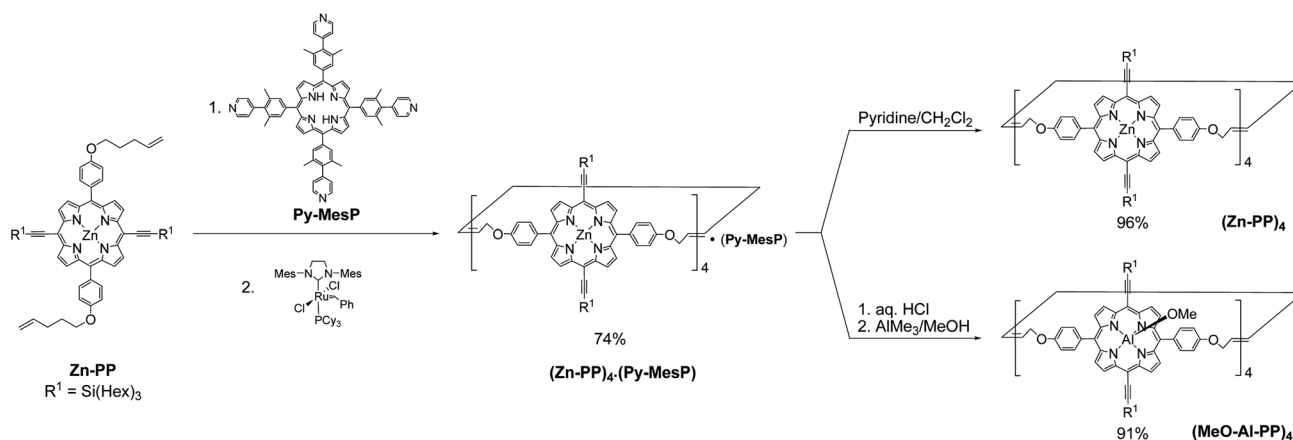


**Fig. 1** <sup>1</sup>H NMR spectra of: (a) **Py-MesP** template, (b) **Zn-PP**, (c) **(Zn-PP)<sub>4</sub>·(Py-MesP)**, (d) **(PP)<sub>4</sub>**, and (e) **(MeO-Al-PP)<sub>4</sub>**. Spectra a–d were obtained in CDCl<sub>3</sub>, whereas spectrum e was obtained in a CDCl<sub>3</sub>/CD<sub>3</sub>OD (8.8 : 1 v/v) solvent mixture due to insufficient solubility of the assembly in CDCl<sub>3</sub>. For a larger version of this figure, please see Fig. S14 in ESI†.



**Scheme 1** Syntheses of porphyrin molecular boxes by tRCM.

precursor by size-exclusion chromatography in a mixture of  $\text{CH}_2\text{Cl}_2/\text{pyridine}$  (9 : 1 v/v). Interestingly, the **Py-MesP** template could not be re-inserted into this hollow assembly, presumably due to geometrical isomers that is generated by some *trans* C=C bonds in the assembly (Fig. S15, ESI<sup>†</sup>). This observation suggests that the initial templation is a less-than-optimal tight fit and *E/Z* isomers make the assembly smaller than usual. However, the smaller template 5,15-bisphenyl-10,20-bis(4-pyridyl)porphyrin (**DPyDPP**) can be easily encapsulated by hollow **(Zn-PP)<sub>4</sub>** (Fig. S15, ESI<sup>†</sup>). The Zn ions in **(Zn-PP)<sub>4</sub>** can be removed by treatment with aq HCl in  $\text{CH}_2\text{Cl}_2$  to yield the free-base assembly **(PP)<sub>4</sub>**, which can be remetalated with  $\text{AlMe}_3$  to provide **(MeO-Al-PP)<sub>4</sub>** in quantitative yield.

The MALDI-ToF mass spectrum of **(Zn-PP)<sub>4</sub>·(Py-MesP)** exhibited two intense molecular ion peaks at  $m/z$  1033.94 and 5116.91 (Fig. 2a), respectively, consistent with the release of **Py-MesP** template from the **(Zn-PP)<sub>4</sub>** cavity before or during the ionization process. While the **(Zn-PP)<sub>4</sub>** assembly does not show significant fragmentation in the presence of a mildly acidic matrix such as dithranol, the **(MeO-Al-PP)<sub>4</sub>** hollow box is much less stable toward demetallation during MALDI-ToF ionization in this matrix: peaks with successive  $\text{AlOMe}$  losses can clearly be observed (see Fig. S10, ESI<sup>†</sup> and the associated discussion). Such progressive demetallation has been previously reported for a cyclic tris(Zn-porphyrin) assembly under MALDI conditions, albeit in the absence of a matrix.<sup>25</sup> In the presence of a neutral pyrene matrix, **(MeO-Al-PP)<sub>4</sub>** is more stable against demetallation: only a molecular ion peak at  $m/z$  5000.05, consistent with loss of two methoxides and one Al atom ( $[\text{M} - \text{AlOMe} - \text{OCH}_3]^+$ ), can be observed together with related species (in order of increasing mass:  $[\text{M} - \text{AlOMe} - \text{CH}_3]^+$ ,  $[\text{M} - \text{AlOMe}]^+$ ,  $[\text{M} - \text{OMe} - \text{CH}_3]^+$ , and  $[\text{M} - \text{OMe}]^+$ , see Fig. 2c). We note that loss of axial ligand is commonly observed for oxophilic metalloporphyrins (*e.g.*,  $\text{Sn}^{\text{IV}}$  or  $\text{Al}^{\text{III}}$ ) under MALDI-ToF MS conditions, especially in the presence of an acidic matrix<sup>26</sup> or a coordinating additive.<sup>27</sup>

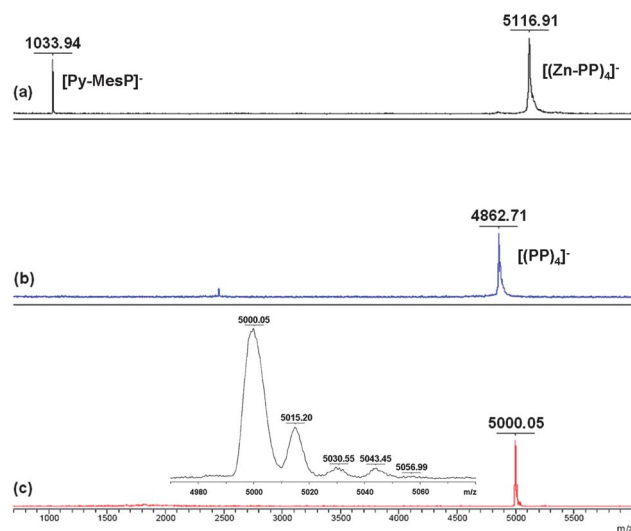


**Fig. 2** MALDI-ToF mass spectra of: (a) **(Zn-PP)<sub>4</sub>·(Py-MesP)**, (b) **(PP)<sub>4</sub>**, and (c) **(MeO-Al-PP)<sub>4</sub>**.

Fortunately, analysis of the **(MeO-Al-PP)<sub>4</sub>** sample by high-resolution electrospray ionization mass spectrometry (HRESIMS) does not result in any demetallation. The ESI mass spectrum of **(MeO-Al-PP)<sub>4</sub>** exhibited two strong peaks at  $m/z$  2512.57 and 2526.57 that are consistent with  $[\text{M} - 2\text{OMe}]^{2+}$  and  $[\text{M} + \text{H} - \text{OMe}]^{2+}$  species (Fig. S12, ESI<sup>†</sup>). The experimentally observed isotopic patterns for both peaks nicely matched the predicted isotopic distribution patterns (Fig. S13, ESI<sup>†</sup>), allowing us to be confident about the structural assignment of **(MeO-Al-PP)<sub>4</sub>**. Additional evidence for the homogeneity and purity of **(MeO-Al-PP)<sub>4</sub>** is provided by its <sup>1</sup>H NMR spectrum (Fig. S9b, ESI<sup>†</sup>): integrating the two aromatic porphyrin β-proton resonances against the broad alkoxy resonance at 4.4 ppm (attributed to the axial  $\text{CH}_3\text{O}$  resonance<sup>27</sup> and the resonance of the  $\text{CH}_2\text{O}$  group in the 4-octenyl linkers) gave the expected 32 : 28 ratio, suggesting a complete metallation of the **(PP)<sub>4</sub>** starting material with  $\text{Al-OMe}$ .

Additional evidence for the formation of the aforementioned tetrakis(metalloporphyrin) assemblies comes from gel-permeation chromatography (GPC) analysis.<sup>16,28</sup> As expected, the GPC retention time is inversely proportional to the assembly size, where **(MeO-Al-PP)<sub>4</sub>** elutes well before **MeO-Al-PP**, and **(Zn-PP)<sub>4</sub>** elutes faster than **Zn-PP**. In addition, the faster elution time of the templated **(Zn-PP)<sub>4</sub>·(Py-MesP)** structure (5.3 min) compared to either the hollow **(Zn-PP)<sub>4</sub>** assembly (5.9 min) or **Zn-PP** monomer (6.9 min) suggests that the templated box is rigidified against distortion (Fig. S19, ESI<sup>†</sup>). Consequently, it spends less time in the pores of the column packing materials than the flexible hollow structure and the smaller monomer.

The apparent hydrodynamic radii of the aforementioned porphyrin box species can also be qualitatively compared using solution-phase pulsed-field-gradient (PFG) NMR measurements<sup>29</sup> (Figs. S20–S24, ESI<sup>†</sup>), following literature precedents.<sup>30–32</sup> As determined using the Stokes–Einstein relation,<sup>33</sup> the calculated hydrodynamic radius of **(MeO-Al-PP)<sub>4</sub>** is slightly larger than that for **(Zn-PP)<sub>4</sub>·(Py-MesP)**, which in turn is larger than that for hollow **(Zn-PP)<sub>4</sub>** (Table 1). All of the boxes are much larger than the corresponding **MeO-Al-PP** and **Zn-PP** monomers.

### Catalytic activity of metalloporphyrin boxes

As mentioned in the introduction, because both **(MeO-Al-PP)<sub>4</sub>** and **(Zn-PP)<sub>4</sub>** contain large hydrophobic cavities with multiple Lewis-acidic metalloporphyrins, we anticipated that they would

**Table 1** Diffusion constants ( $D_s$ ) and calculated hydrodynamic radii ( $a$ ) for the porphyrin box species<sup>a</sup>

Porphyrin species	Diffusion constant, $D_s/10^{-10} \text{ m}^2 \text{ s}^{-1}$	Hydrodynamic radius, $a/\text{Å}$
<b>Zn-PP</b>	$5.41 \pm 0.12$	$7.2 \pm 0.2$
<b>(Zn-PP)<sub>4</sub></b>	$2.57 \pm 0.02$	$15.1 \pm 0.1$
<b>(Zn-PP)<sub>4</sub>·(Py-MesP)</b>	$2.51 \pm 0.02$	$15.5 \pm 0.1$
<b>MeO-Al-PP</b>	$4.23 \pm 0.12$	$9.2 \pm 0.3$
<b>(MeO-Al-PP)<sub>4</sub></b>	$2.43 \pm 0.09$	$16.0 \pm 0.6$

<sup>a</sup> All NMR diffusion measurements were performed on 3.2-mM samples at 298 K in either  $\text{CDCl}_3$  (Zn species) or (to enhance solubility) a  $\text{CDCl}_3/\text{CD}_3\text{OD}$  (8.8 : 1 v/v) solvent mixture (Al species).

be good catalysts for the methanolysis of phosphate triesters in the presence of a high methanol concentration. We anticipated that the methanol reagent and the relatively hydrophobic phosphate substrate might be simultaneously bound inside the cavity of these supramolecular assemblies, leading to enhanced reactivity. The alcoholysis of phosphate triesters, particularly methanolysis, has important implications for the degradation of phosphate-type nerve agents<sup>34</sup> and the decomposition of biologically relevant phosphate diesters such as the nucleic acids.<sup>35</sup> The acceleration of such reactions has been extensively investigated by Brown and co-workers using a wide range of Lewis-acidic metal ions such as  $\text{La}^{3+}$ ,<sup>36</sup>  $\text{Cu}^{2+}$ ,<sup>37</sup> and  $\text{Zn}^{2+}$  as catalysts.<sup>38</sup> In Nature, however, organophosphorus hydrolases (OPHs), enzymes that promote the hydrolysis of phosphate esters, often possess active sites containing two  $\text{Zn}^{\text{II}}$  ions where one metal coordinates the substrate, which then undergoes intramolecular attack by a hydroxide coordinated to the second metal (Fig. 3).<sup>39</sup> Thus, we reasoned that the cavities of the  $(\text{Zn-PP})_4$  and  $(\text{MeO-Al-PP})_4$  assemblies (Fig. 4), with their multiple metal centers, might well provide environments that mimic, at least conceptually, the active sites of OPHs. While the dianionic porphyrin ligand environment prevents the  $\text{Zn}^{\text{II}}$  centers from  $(\text{Zn-PP})_4$  to carry methoxide ions, the  $\text{Al}^{\text{III}}$  centers in  $(\text{MeO-Al-PP})_4$  can deliver a bolus of this nucleophile to the local environment around this latter assembly and should be more active catalytically. The hydrophobic environment of the free-base  $(\text{PP})_4$  assembly then would serve as a convenient control to allow us to evaluate the effect of solvophobic encapsulation alone.

The catalytic methanolysis of *p*-nitrophenyl diphenyl phosphate (PNPDPP), a common simulant for nerve agents,<sup>40</sup> was carried out in the presence of catalytic amounts of each of several porphyrin species.  $(\text{MeO-Al-PP})_4$  is highly active for this reaction, showing a  $\sim 120$ -fold rate enhancement relative to the  $\text{MeO-Al-PP}$  monomer and is  $\sim 430$  times faster than the uncatalyzed reaction, converting 50% of the PNPDPP substrate within 10 h (Fig. 5 and Table S1 in ESI†). As expected, the use of  $(\text{Zn-PP})_4$  as a catalyst results in a much-lower rate than with the  $(\text{MeO-Al-PP})_4$  assembly, reaching only 12% conversion after 59 h. However, this is still 5 times greater than the rate obtained with the corresponding  $\text{Zn-PP}$  monomer (Table S1 in ESI†) and 14 times faster than the rate of the uncatalyzed reactions.

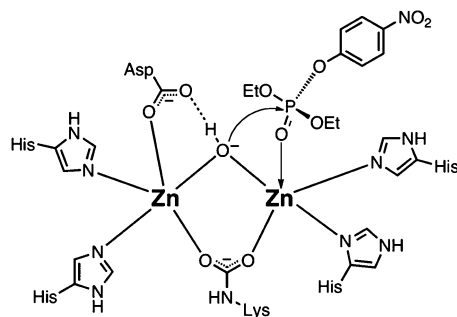


**Fig. 3** A proposed structure for the hydrolysis of a phosphate triester in the active site of a phosphotriesterase enzyme. Adapted from ref. 39.

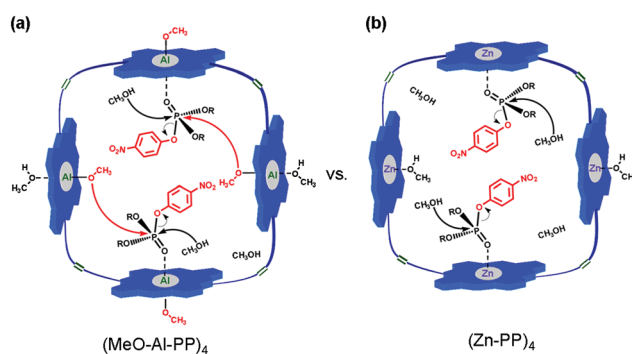


**Fig. 4** Proposed catalytic methanolysis of phosphate triesters in the cavity of: (a)  $(\text{MeO-Al-PP})_4$  and (b)  $(\text{Zn-PP})_4$ . The “box-like” geometry drawn herein for both isomers is idealized to focus the readers on the bimolecular catalysis processes inside the cavities. In reality, both structures are much more flexible and far from being box-like given the 4-octen-1,8-diyl linkages between the porphyrins. The *E/Z* isomerism within the 4-octen-1,8-diyl linkages additionally gave rise to six different geometrical isomers for each structure, many of which are elongated in shapes (see Fig. S16 and the associated discussion in ESI†).

### Proposed mechanism

The metal center in zinc porphyrin is well-known to bind one additional axial ligand and become five-coordinate.<sup>41</sup> If a phosphate ester becomes encapsulated within  $(\text{Zn-PP})_4$  and subsequently activated by a Lewis-acidic  $\text{Zn}^{\text{II}}$  center, it can undergo accelerated methanolysis by reacting with free methanol in the supramolecular assembly (black arrows in Fig. 4b) or with other alcohol nucleophiles that are coordinated to the remaining  $\text{Zn}^{\text{II}}$  centers. However, the oxygen atom of a methanol coordinated to  $\text{Zn}^{\text{II}}$  metal sites is much less nucleophilic than that of free methanol<sup>42</sup> and presumably would not be a significant contributor.

In an attempt to confirm the Lewis acid activation of PNPDPP in  $(\text{Zn-PP})_4$ , the methanolysis of PNPDPP was carried out with 3

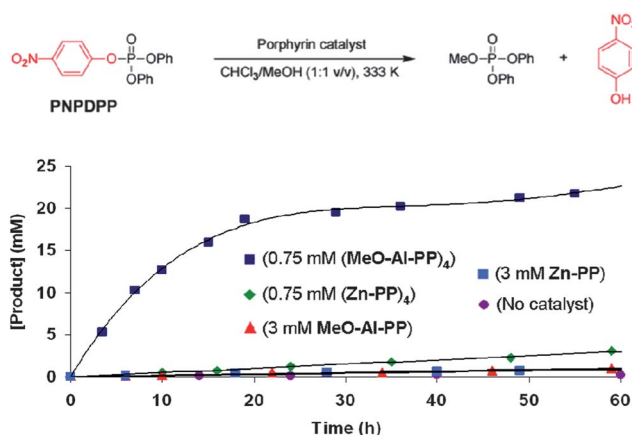


**Fig. 5** Reaction profiles for the methanolysis of PNPDPP (25 mM) carried out at 333 K, in  $\text{CHCl}_3/\text{CH}_3\text{OH}$  (1 : 1 v/v) and in the presence of: (■) 0.75 mM  $(\text{MeO-Al-PP})_4$ , (◆) 0.75 mM  $(\text{Zn-PP})_4$ , (▲) 3 mM  $\text{MeO-Al-PP}$ , (■) 3 mM  $\text{Zn-PP}$ , and (●) no catalyst. The product was monitored by  $^{31}\text{P}$  NMR spectroscopy. For a larger version of this figure, please see Fig. S26 in ESI†.

mol% of demetallated **(PP)**<sub>4</sub> in CHCl<sub>3</sub>/CH<sub>3</sub>OH (1 : 1 v/v) at 333 K. The initial reaction rate for PNPDP methanolysis in the presence of **(PP)**<sub>4</sub> is three times lower than that for the corresponding **Zn-PP** monomer and much slower than that for **(Zn-PP)**<sub>4</sub> (Table S1, ESI†). That this rate is nearly the same as the rate of the uncatalyzed reactions confirms the presence of the Lewis acidic Zn<sup>II</sup> ions, whether in **(Zn-PP)**<sub>4</sub> or **Zn-PP**, as being essential for enhanced catalysis. Presumably, the methanolysis of the phosphate triester substrate is enhanced if it is first activated by coordinating to the Lewis-acidic Zn<sup>II</sup> centers.

In the case of **(MeO-Al-PP)**<sub>4</sub>, the ability of (porphyrin)Al<sup>III</sup> to coordinate an additional sixth oxygen ligand<sup>43–45</sup> also affords a methanolysis-by-free-methanol mechanism (black arrows in Fig. 4a). However, the presence of an *additional* axial methoxide ligand per Al center led us to believe that a phosphate ester encapsulated and activated by the **(MeO-Al-PP)**<sub>4</sub> assembly would be able to access an additional, *even faster* methanolysis pathway by reacting with the methoxide nucleophiles that are coordinated to the remaining Al<sup>III</sup> centers (red arrows in Fig. 4a). The supramolecular effect in catalysis by **(MeO-Al-PP)**<sub>4</sub> is accentuated by the observation that **(MeO-Al-PP)**<sub>4</sub> is ~30 times more active than the **(Zn-PP)**<sub>4</sub> assembly. Such differences in rate acceleration are best explained as arising from a high *local* concentration of methoxide within the cavity of **(MeO-Al-PP)**<sub>4</sub> that would *not* be present for either the **MeO-Al-PP** monomer or the **(Zn-PP)**<sub>4</sub> assembly.

That the **MeO-Al-PP** monomer shows a methanolysis rate that is similar to that of **Zn-PP** monomer (1.2 vs. 1, respectively, Table S1, ESI†) suggests that the methanolysis catalyzed by both monomers is primarily attributable to free methanol, which attacks PNPDP substrates coordinating to Lewis-acidic Al<sup>III</sup> or Zn<sup>II</sup> centers (Figs. S27a and b, ESI†). The aforementioned small difference in rate can partly be ascribed to the slightly higher Lewis acidity of Al<sup>III</sup> compared to Zn<sup>II</sup>. This hypothesis is supported by the slightly larger (~1.6-fold) binding constant of PNPDP ( $K_{\text{a(PNPDP)}}$ ) to **MeO-Al-PP** monomer than to **Zn-PP** monomer (Table 2), as measured by fluorescence titration (Figs. S39 and S40, ESI†). The other component responsible for the higher catalysis rate by **MeO-Al-PP** would be the presence of the axial methoxide, which can attack PNPDP, both free and coordinated. The methanolysis of PNPDP by (porphyrin)M-coordinated methanol (Path 1 in Figs. S27a and b, ESI†) is expected to be a very small contribution to the overall rate for both monomers, a consequence of the reduced nucleophilicity of the coordinated alcohol.

**Table 2** Experimental and predicted<sup>46</sup> binding constants ( $K_{\text{a}}$ ) for PNPDP of porphyrin species in CHCl<sub>3</sub>/CH<sub>3</sub>OH (1 : 1 v/v) at 296 K

Porphyrin species	Experimental $K_{\text{a}}^{\text{a}}/\text{M}^{-1}$	Predicted $K_{\text{a}}^{\text{b}}/\text{M}^{-1}$
<b>Zn-PP</b>	<3	—
<b>MeO-Al-PP</b>	4.5 ± 0.6	—
<b>(Zn-PP)</b> <sub>4</sub>	17.3 ± 0.7	4.3 ± 0.3
<b>(MeO-Al-PP)</b> <sub>4</sub>	26.9 ± 2.6	5.3 ± 0.3

<sup>a</sup> Fluorescence titration experiments of PNPDP were carried out on 0.02 μM solution of the porphyrin tetramers and 0.04 μM solution of the porphyrin monomers. <sup>b</sup> See section XII in ESI† for a detailed calculation of the predicted  $K_{\text{a}}$  values and their standard errors.

### High local concentration of methoxide in the vicinity of **(MeO-Al-PP)**<sub>4</sub>

The significance of the high local methoxide concentration in the vicinity of the **(MeO-Al-PP)**<sub>4</sub> assembly is immediately apparent from comparing the methoxide concentrations localized at the **(MeO-Al-PP)**<sub>4</sub> assembly and the **MeO-Al-PP** monomer (Fig. S29, ESI†). As estimated in section IX of ESI†, the local concentration of methoxide in the vicinity of the **(MeO-Al-PP)**<sub>4</sub> assembly (0.33–0.6 M) is ~110–200 times the concentration of methoxide near the **MeO-Al-PP** monomer (0.003 M), suggesting that the former is a major contributor to the observed rate acceleration in the methanolysis of PNPDP by **(MeO-Al-PP)**<sub>4</sub>. Additional support for this idea is provided by the ~125 M effective molarity (EM)<sup>47</sup> value calculated for the methanolysis of PNPDP catalyzed by **(MeO-Al-PP)**<sub>4</sub> (see section IX of ESI†). That this value is in the same range as the 110–200 fold higher local methoxide concentration for the tetramer assembly (in comparison to the monomer) agrees well with the geometrical estimate. We note that the local methoxide ion concentrations for both the tetramer and monomer are several orders of magnitude greater than the methoxide concentration in pure MeOH (4.5 × 10<sup>-9</sup> M, calculated from its autoprotolysis constant, see section IX in ESI†).

Because **(MeO-Al-PP)**<sub>4</sub> and **(Zn-PP)**<sub>4</sub> have essentially the same structures except for the identity of the central metal ion and the axial methoxide ligand, we would expect the local concentrations of Lewis-acidic sites to be the same. Indeed, the 1.6 ratio of  $K_{\text{a(PNPDP)}}$  values for **(MeO-Al-PP)**<sub>4</sub> relative to **(Zn-PP)**<sub>4</sub> is essentially the same as that for the corresponding monomers (Table 2). Taken together with the aforementioned estimates of local methoxide ion concentrations, these data suggest that the observed ~30-fold rate enhancement for **(MeO-Al-PP)**<sub>4</sub> relative to **(Zn-PP)**<sub>4</sub> is primarily a consequence of the high local [OMe] available with **(MeO-Al-PP)**<sub>4</sub>.

The versatility of tetrakis(metalloporphyrin) assemblies in the catalytic methanolysis of phosphate triesters can be extended to a wide range of *p*-nitrophenyl dialkyl phosphates. Consistent with a methoxide-induced mechanism, the **(MeO-Al-PP)**<sub>4</sub>-catalyzed methanolysis of *p*-nitrophenyl dimethyl phosphate (PNPDMP) is 2.5 times faster than that of *p*-nitrophenyl dipropyl phosphate (PNPDPrP) and 3 times faster than that of *p*-nitrophenyl dibutyl phosphate (PNPDBP) (Table S2, ESI†). This is similar to the typically observed order of reactivity for the hydrolysis of phosphate triesters in the presence of base,<sup>48</sup> where steric encumbrance of the phosphorus center can retard the reaction rate. In contrast, other metalloporphyrin species show nearly identical reaction rates for the methanolysis of different *p*-nitrophenyl dialkyl phosphates (~1 × 10<sup>-8</sup> M<sup>-1</sup> s<sup>-1</sup> for **(Zn-PP)**<sub>4</sub>, ~2 × 10<sup>-9</sup> M<sup>-1</sup> s<sup>-1</sup> for **Zn-PP** monomer, and ~3 × 10<sup>-9</sup> M<sup>-1</sup> s<sup>-1</sup> for **MeO-Al-PP** monomer, respectively, Tables S3 and S4, ESI†) that is typical of a Lewis-acid-activation mode.

### Solvophobic encapsulation of the PNPDP substrate by **(MeO-Al-PP)**<sub>4</sub> and **(Zn-PP)**<sub>4</sub>

Interestingly, at high concentrations of MeOH, the ratio of the PNPDP methanolysis rates in the presence of **(MeO-Al-PP)**<sub>4</sub>, vs. **MeO-Al-PP**, skews further in favor of the tetramer (Fig. 6

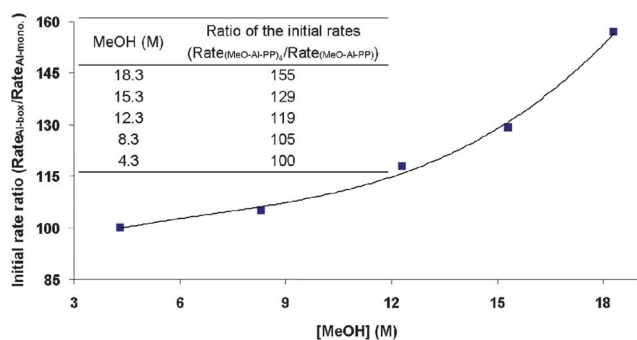


**Fig. 6** The ratio of product formation rates between **(MeO-Al-PP)<sub>4</sub>** and **MeO-Al-PP** at various MeOH concentrations. Reported catalyzed rates were background-corrected from uncatalyzed reactions.

and Table S5, ESI†). This observation implies that the even faster increase of the initial rate with **(MeO-Al-PP)<sub>4</sub>** could be a result of stronger binding of the hydrophobic PNPDP in the cavity of **(MeO-Al-PP)<sub>4</sub>** as the hydrophilicity of the solvent is increased. Indeed, it was observed that the binding constant of PNPDP for **(MeO-Al-PP)<sub>4</sub>** is  $\sim 3$ -fold larger than that for **MeO-Al-PP** monomer in pure  $\text{CHCl}_3$  (see section XII in ESI†) but becomes 6-fold larger in a 1 : 1 v/v  $\text{CHCl}_3/\text{CH}_3\text{OH}$  solvent mixture (Table 2). Considering that the predicted  $K_{\text{a(PNPDP)}}$  of **(MeO-Al-PP)<sub>4</sub>** in this solvent mixture appears to be negligible ( $5.3 \text{ M}^{-1}$ , Table 2), it is clear that there is a component of the experimentally observed binding constant ( $26.9 \text{ M}^{-1}$ , Table 2) that is not based on simple Lewis acid–Lewis base interactions. We attribute this extra component to the solvophobic encapsulation of the relatively hydrophobic PNPDP substrate by **(MeO-Al-PP)<sub>4</sub>**, which increases as the concentration of hydrophilic MeOH increases outside the cavity (Fig. 7b). Interestingly, such a mechanism has been used by Moore and co-workers to elucidate the binding of monoterpenes inside *mPE* foldamers in a mixture of  $\text{H}_2\text{O}/\text{CH}_3\text{CN}$ <sup>49</sup> but has not been associated with a supramolecular catalytic system in a solvent mixture. We note that while many examples of enhanced catalysis *via* hydrophobic supramolecular encapsulation effect have been reported,<sup>50–54</sup> these studies have often been carried out in single-component solvents and not in a mixture of organic solvents as reported herein. For

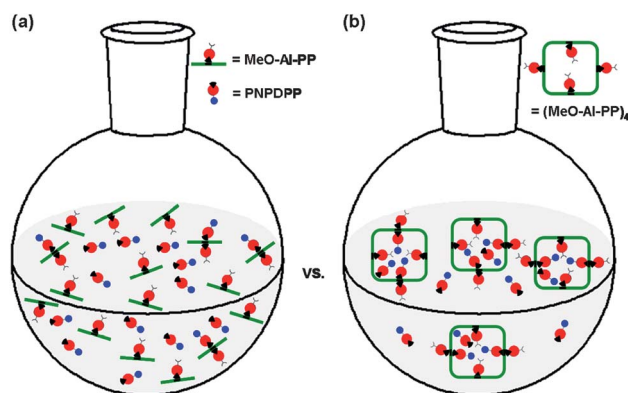


**Fig. 7** Schematic description of the solvophobic encapsulation of PNPDP in the presence of: (a) **MeO-Al-PP** and (b) **(MeO-Al-PP)<sub>4</sub>** in a  $\text{CHCl}_3/\text{CH}_3\text{OH}$  (1 : 1 v/v) solvent mixture.

supramolecules with large cavities such as those reported in this work, solvophobic effects play an important role at high MeOH concentrations by boosting the binding constant for PNPDP encapsulation.

That the experimental  $K_{\text{a(PNPDP)}}$  of **(Zn-PP)<sub>4</sub>** is much higher than the predicted  $K_{\text{a(PNPDP)}}$  (Table 2) clearly points to the existence of the solvophobic effect in **(Zn-PP)<sub>4</sub>** under the catalysis conditions. Interestingly, the  $\sim 6$ -fold higher  $K_{\text{a(PNPDP)}}$  for **(Zn-PP)<sub>4</sub>** vs. **Zn-PP** monomer in a 1 : 1 v/v  $\text{CHCl}_3/\text{CH}_3\text{OH}$  solvent mixture (Table 2) is well-matched to the observed  $\sim 5$ -fold enhancement in reaction rate. This implies that the stronger binding of PNPDP inside the cavity, whether by Lewis-acid activation or solvophobic encapsulation, is a major contributor to the observed rate acceleration in the methanolysis of PNPDP by **(Zn-PP)<sub>4</sub>**.<sup>55</sup>

Unfortunately, our attempts to observe the solvophobic encapsulation of PNPDP in **(MeO-Al-PP)<sub>4</sub>** or **(Zn-PP)<sub>4</sub>** using variable-temperature (VT) and PFG NMR spectroscopies,<sup>56</sup> were not successful. While Ballester and co-workers were able to identify separate signals in 1D and PFG NMR spectra for the inclusion of trimethylphosphine oxide in a tightly closed tetraurea calix[4]pyrrole host,<sup>57</sup> we were unable to detect distinct resonances for the encapsulated PNPDP under a wide range of conditions (section XIII in ESI†). These observations suggest that the exchange of PNPDP between solution and the open tetrakis(porphyrin) cavities is too rapid to be observed under the conditions of our experiments.

## Conclusions

In summary, we find that covalently linked hollow metal-porphyrin boxes possessing tunable Lewis-acidic metal sites can substantially catalyze the methanolysis of phosphate triesters. Tuning the active sites inside the cavities of these large tetramers,<sup>58</sup> such as replacing the Zn centers in the multiporphyrin assembly with Al-OMe moieties, affords a new nucleophilic environment where a high concentration of methoxy ligands becomes available for enhanced reaction with encapsulated phosphate triester. This combination of increased local nucleophilicity and supramolecular encapsulation effect is reminiscent of certain features in enzymatic systems and points to the vast potential that mimicking biological design can bring to supramolecular catalysis.

## Acknowledgements

This material is based upon research sponsored by the Air Force Office of Scientific Research, under agreement FA-9550-07-1-0534. We acknowledge DTRA (grant #HDTRA1-10-0023) for additional financial support of this work. We thank Dr. Chul Hoon Kim for initial help with the fitting of titration data using OriginPro 8.0 software. We additionally thank the reviewers of a previous version of this manuscript and the reviewers for this version for inputs that greatly strengthened our work.

## Notes and references

- 1 M. Yoshizawa, J. K. Klosterman and M. Fujita, *Angew. Chem., Int. Ed.*, 2009, **48**, 3418–3438.

- 2 D. Fiedler, D. H. Leung, R. G. Bergman and K. N. Raymond, *Acc. Chem. Res.*, 2005, **38**, 349–358.
- 3 W. B. Motherwell, M. J. Bingham and Y. Six, *Tetrahedron*, 2001, **57**, 4663–4686.
- 4 Y. Murakami, J.-i. Kikuchi, Y. Hisaeda and O. Hayashida, *Chem. Rev.*, 1996, **96**, 721–758.
- 5 I. Beletskaya, V. S. Tyurin, A. Y. Tsivadze, R. Guilard and C. Stern, *Chem. Rev.*, 2009, **109**, 1659–1713.
- 6 K. S. Suslick and S. van Deussen-Jeffries, in *Comprehensive Supramolecular Chemistry*, eds. J. L. Atwood, J. E. D. Davies, D. D. MacNicol and F. Vögtle, Pergamon, New York, 1996, vol. 5, pp. 141–170.
- 7 W. D. Woggon, *Acc. Chem. Res.*, 2005, **38**, 127–136.
- 8 S. J. Lee and J. T. Hupp, *Coord. Chem. Rev.*, 2006, **250**, 1710–1723.
- 9 S. J. Lee, S. H. Cho, K. L. Mulfort, D. M. Tiede, J. T. Hupp and S. T. Nguyen, *J. Am. Chem. Soc.*, 2008, **130**, 16828–16829.
- 10 M. Kuil, T. Soltner, P. W. N. M. van Leeuwen and J. N. H. Reek, *J. Am. Chem. Soc.*, 2006, **128**, 11344–11345.
- 11 V. F. Slagt, P. C. J. Kamer, P. W. N. M. van Leeuwen and J. N. H. Reek, *J. Am. Chem. Soc.*, 2004, **126**, 1526–1536.
- 12 L. G. Mackay, R. S. Wylie and J. K. M. Sanders, *J. Am. Chem. Soc.*, 1994, **116**, 3141–3142.
- 13 M. L. Merlau, M. D. P. Mejia, S. T. Nguyen and J. T. Hupp, *Angew. Chem., Int. Ed.*, 2001, **40**, 4239–4242.
- 14 C. G. Oliveri, N. C. Gianneschi, S. T. Nguyen, C. A. Mirkin, C. L. Stern, Z. Wawrzak and M. Pink, *J. Am. Chem. Soc.*, 2006, **128**, 16286–16296.
- 15 C. J. Walter, H. L. Anderson and J. K. M. Sanders, *J. Chem. Soc., Chem. Commun.*, 1993, 458–460.
- 16 K.-T. Youm, S. T. Nguyen and J. T. Hupp, *Chem. Commun.*, 2008, 3375–3377.
- 17 J. M. Bakker, S. J. Langford, M. J. Latter, K. A. Lee and C. P. Woodward, *Aust. J. Chem.*, 2005, **58**, 757–761.
- 18 P. C. M. van Gerven, J. A. A. W. Elemans, J. W. Gerritsen, S. Speller, R. J. M. Nolte and A. E. Rowan, *Chem. Commun.*, 2005, 3535–3537.
- 19 T. Ishida, Y. Morisaki and Y. Chujo, *Tetrahedron Lett.*, 2006, **47**, 5265–5268.
- 20 A. M. Shultz, O. K. Farha, J. T. Hupp and S. T. Nguyen, *J. Am. Chem. Soc.*, 2009, **131**, 4204–4205.
- 21 W. P. Jencks, *Catalysis in Chemistry and Enzymology*, McGraw-Hill, New York, 1969.
- 22 D. Astruc, *New J. Chem.*, 2005, **29**, 42–56.
- 23 S. Anderson, H. L. Anderson, A. Bashall, M. McPartlin and J. K. M. Sanders, *Angew. Chem., Int. Ed.*, 1995, **34**, 1096–1099.
- 24 E. B. Fleischer and A. M. Shachter, *Inorg. Chem.*, 1991, **30**, 3763–3769.
- 25 E. Stulz, C. C. Mak and J. K. M. Sanders, *J. Chem. Soc., Dalton Trans.*, 2001, 604–613.
- 26 M. J. Crossley, P. Thordarson and R. A. S. Wu, *J. Chem. Soc., Perkin Trans. 1*, 2001, 2294–2302.
- 27 G. A. Metselaar, J. K. M. Sanders and J. de Mendoza, *Dalton Trans.*, 2008, 588–590.
- 28 C. R. Graves, M. L. Merlau, G. A. Morris, S. T. Sun, S. T. Nguyen and J. T. Hupp, *Inorg. Chem.*, 2004, **43**, 2013–2017.
- 29 W. S. Price, *Concepts Magn. Reson.*, 1998, **10**, 197–237.
- 30 W. H. Otto, M. H. Keefe, K. E. Splan, J. T. Hupp and C. K. Larive, *Inorg. Chem.*, 2002, **41**, 6172–6174.
- 31 P. Timmerman, J.-L. Weidmann, K. A. Jolliffe, L. J. Prins, D. N. Reinhoudt, S. Shinkai, L. Frish and Y. Cohen, *J. Chem. Soc., Perkin Trans. 2*, 2000, 2077–2089.
- 32 B. Olenyuk, M. D. Levin, J. A. Whiteford, J. E. Shield and P. J. Stang, *J. Am. Chem. Soc.*, 1999, **121**, 10434–10435.
- 33 J. P. Hansen and I. R. McDonald, *Theory of Simple Liquids*, Academic Press, London, 1976, ch. 8.
- 34 B. M. Smith, *Chem. Soc. Rev.*, 2008, **37**, 470–478.
- 35 A. A. Neverov and R. S. Brown, *Inorg. Chem.*, 2001, **40**, 3588–3595.
- 36 D. R. Edwards, C. T. Liu, G. E. Garrett, A. A. Neverov and R. S. Brown, *J. Am. Chem. Soc.*, 2009, **131**, 13738–13748.
- 37 C. T. Liu, A. A. Neverov, C. I. Maxwell and R. S. Brown, *J. Am. Chem. Soc.*, 2010, **132**, 3561–3573.
- 38 C. T. Liu, A. A. Neverov and R. S. Brown, *J. Am. Chem. Soc.*, 2008, **130**, 16711–16720.
- 39 K.-Y. Wong and J. Gao, *Biochemistry*, 2007, **46**, 13352–13369.
- 40 H. Morales-Rojas and R. A. Moss, *Chem. Rev.*, 2002, **102**, 2497–2521.
- 41 G. M. Mamardashvili, N. Z. Mamardashvili and O. I. Koifman, *Russ. Chem. Rev.*, 2005, **74**, 765–780.
- 42 We note that the situation here is different from the Zn dimer case shown in Fig. 3. There, the OH nucleophile is positioned next to the Asp residue, which acts as an internal base to ionize the proton of the OH moiety and induce a negative charge on the remaining oxygen, thus increases its nucleophilicity for the subsequent attack to the coordinated phosphate ester. This scenario does not exist for our catalysts. While coordination of methanol to a Lewis-acidic (porphyrin)metal center can indeed increase the acidity of the methanol, the coordinated oxygen will not be very nucleophilic toward the external phosphate ester.
- 43 S. Richeter, J. Thion, A. van der Lee and D. Leclercq, *Inorg. Chem.*, 2006, **45**, 10049–10051.
- 44 Y. Watanabe, T. Yasuda, T. Aida and S. Inoue, *Macromolecules*, 1992, **25**, 1396–1400.
- 45 K. Shimasaki, T. Aida and S. Inoue, *Macromolecules*, 1987, **20**, 3076–3080.
- 46 In the calculation of the predicted  $K_a$ , we assume that the solvent environment for a  $\text{CHCl}_3/\text{MeOH}$  (1 : 1 v/v) solvent mixture is the same as that in pure  $\text{CHCl}_3$ . If we have to predict the binding constant for PNPDP in 1 : 1 v/v methanol/chloroform based on accessible experimental data, there is no easy way for us to accomplish this task without making the aforementioned assumption. The need to make such an assumption is actually a point that we want to make in this paper: the predicted values turned out to be much lower than the experimental values because they require an assumption that ignores the different solvent environment, and thus the solvophobic encapsulation effect, in the 1 : 1 v/v methanol/chloroform mixture.
- 47 R. Cacciapaglia, S. Di Stefano and L. Mandolini, *Acc. Chem. Res.*, 2004, **37**, 113–122.
- 48 S. C. Jao, L. F. Huang, Y. S. Tao and W. S. Li, *J. Mol. Catal. B: Enzym.*, 2004, **27**, 7–12.
- 49 R. B. Prince, S. A. Barnes and J. S. Moore, *J. Am. Chem. Soc.*, 2000, **122**, 2758–2762.
- 50 *Molecular Encapsulation: Organic Reactions in Constrained Systems*, eds. U. H. Brinker and J.-L. Miesusset, John Wiley and Sons, Ltd., Chichester, West Sussex, UK, 2010.
- 51 D. C. Rideout and R. Breslow, *J. Am. Chem. Soc.*, 1980, **102**, 7816–7817.
- 52 L. Barr, C. J. Easton, K. Lee, S. F. Lincoln and J. S. Simpson, *Tetrahedron Lett.*, 2002, **43**, 7797–7800.
- 53 M. D. Pluth, R. G. Bergman and K. N. Raymond, *Science*, 2007, **316**, 85–88.
- 54 Y. B. Zhou, E.-H. Ryu, Y. Zhao and L. K. Woo, *Organometallics*, 2007, **26**, 358–364.
- 55 We note that micelle formation of PNPDP does not occur at the temperature of the reaction even though some micellar formation can be observed by dynamic light scattering at room temperature.
- 56 A. Pastor and E. Martínez-Viviente, *Coord. Chem. Rev.*, 2008, **252**, 2314–2345.
- 57 G. Gil-Ramírez, M. Chas and P. Ballester, *J. Am. Chem. Soc.*, 2010, **132**, 2520–2521.
- 58 Whereas our tetramer assemblies can accommodate more than one PNPDP molecule, smaller porphyrin dimers can only bind one PNPDP molecule in their cavities. See R. K. Totten, P. Ryan, B. Kang, S. J. Lee, L. J. Broadbelt, R. Q. Snurr, J. T. Hupp and S. T. Nguyen, *Chem. Commun.*, 2012, **48**, DOI: 10.1039/c2cc17568a.